ELSEVIER

Tissue & Cell 36 (2004) 197–210

Tissue&Cell

www.elsevier.com/locate/tice

Autoschizis: a new form of cell death for human ovarian carcinoma cells following ascorbate:menadione treatment Nuclear and DNA degradation

Jacques Gilloteaux [a,b,*], James M. Jamison [b], Heather E. Lorimer [c], David Jarjoura [d], Henryk S. Taper [e], Pedro B. Calderon [e], Deborah R. Neal [b], Jack L. Summers [b]

[a] *Department of Anatomy, American University of the Caribbean, School of Medicine, Campus St. Maarten, M.E.I.O. Inc., Ponce de Leon Boulevard 901, Suite #401, Coral Gables, FL 33135, USA*

[b] *Department of Urology, Summa Research Foundation, Summa Health System, Akron, OH 44304, USA*

[c] *Department of Biological Sciences, Youngstown State University, Youngstown, OH 44555, USA*

[d] *Office of Biostatistics, Division of Community Health Sciences, NE Ohio, Universities College of Medicine, Rootstown, OH 44272, USA*

[e] *Unit of Pharmacokinetics, Metabolism, Nutrition and Toxicology, Université Catholique de Louvain, Brussels-Woluwé 1200, Belgium*

Received 25 May 2003; received in revised form 20 January 2004; accepted 27 January 2004

Abstract

Microscopic aspects, densitometric evaluation of Feulgen-stained DNA, and gel electrophoresis of total DNA have been used to elucidate the effects of 1, 2, and 3 h VC (ascorbic acid), VK_3 (menadione), and combined VC:VK_3 treatments on the cellular and nuclear morphology and DNA content of a human ovarian carcinoma cell line (MDAH 2774). Optical densitometry showed a significant decrease in cancer cell DNA content directly related to VC and VC:VK_3 treatments while VK_3 and VC:VK_3 treated cells exhibited cytoskeletal changes that included self-excision of cytoplasmic pieces with no membranous organelles. Nuclei decreased in size and exhibited poor contrast consistent with progressive decondensation of their chromatin. Degraded chromatin was also detected in cytoplasmic autophagosomes. Nucleoli segregated their components and fragmented into small pieces. Gel electrophoretic analysis of total DNA revealed evidence of generalized DNA degradation specific to treated tumor cells. These results are consistent with previous observations [Scanning 20 (1998a) 564; Ultrastruct. Pathol. 25 (2001b) 183; J. Histochem. Cytochem. 49 (2001) 109] which demonstrated that the VC:VK_3 combination induced autoschizic cell death by a series of cytoplasmic excisions without organelles along with specific nuclear ultrastructural damage.

Keywords: Ovarian carcinoma; DNA; Microscopy; Nucleus; Ascorbate; Menadione; Cell death

1. Introduction

An estimated 25,400 new neoplasms of the ovary will be diagnosed during 2003 in the United States. This figure represents about 5% of new female cancer cases (Jemal et al., 2003). Ovarian cancer occurs in American women with an incidence rate of 9.4 cases per 100,000 for those under 65 years of age and an incidence of 54.8 cases per 100,000 after the age of 65 years. Because of its late detection, ovarian carcinoma is among the 10 most lethal malignancies with only 50% of cancer patients surviving 5 years after treatment (Ries, 1993).

Taper and coworkers (Taper et al., 1971, 1987, 1992, 1996; Noto et al., 1989; De Loecker et al., 1993; Calderon et al., 2002) demonstrated that co-administration of sodium ascorbate (Vitamin C or VC) and 2-methyl-1,4-naphthoquinone (Vitamin K_3 or VK_3) to a variety of carcinoma cell lines and tumors in a VC:VK_3 ratio of 100:1 resulted in equivalent antineoplastic activity at concentrations that were 10–50 times lower than when either vitamin was administered alone. Daoust and Taper have shown these tumors exhibit a characteristic loss of one or more DNases and RNases and these nucleases could be reactivated by a number of agents, including Vitamins C and K_3 (Daoust and Amano, 1963; Taper, 1967, 1980). Selective and sequential reactivation of DNase I by VK_3 and DNase II by VC, when the vitamins were administered in combination, resulted in synergistic degradation of DNA and tumor regression (Taper et al., 1987, 2001) and has been implicated along with oxidative stress resulting

* Corresponding author. Tel.: +1-599-545-2298; fax: +1-599-545-2440.
E-mail address: jagillot@yahoo.com (J. Gilloteaux).

0040-8166/$ – see front matter © 2004 Elsevier Ltd. All rights reserved.
doi:10.1016/j.tice.2004.01.006

from the redox cycling of the vitamins in the mechanism of action of the vitamin combination. The subsequent production of reactive oxygen species (ROS) and the concomitant damage to membranes and other lipid-rich cell structures, along with the oxidation of sulfhydryl (–SH) groups and depletion of reduced glutathione (Begleiter, 1983; Carbonera and Azzone, 1988) produce irreversible damage in the cancer cells which leads to autoschizis (Gilloteaux et al., 1998a,b; Ervin et al., 1998; Jamison et al., 2002).

Autoschizis exhibits a unique set of morphological and biomolecular alterations that distinguish it from apoptosis and oncosis (Gilloteaux et al., 1998a,b, 1999, 2001a,b,c,d, 2003a,b; Taper et al., 2001; Jamison et al., 1996, 2001, 2002). Specifically, in bladder and prostate cancer cells, cytoplasmic self-excisions and the associated nuclear changes result in the diminution of cell size, the disappearance of chromatin from nucleolus and nucleoplasm and subsequent nucleolar compaction and fragmentation during karyorrhexis and karyolysis. During these events, DNA is degraded in a random fashion similar to that occurring during necrosis. The purpose of this report is to characterize the histochemical and related cytological and ultrastructural changes in MDAH 2774 human ovarian carcinoma cells following their exposure to the vitamins.

2. Materials and methods

2.1. Cell lines

Human foreskin fibroblasts were purchased from Bio-Whittaker (MHRF, Walkersville, MD). Human ovarian carcinoma cells (MDAH 2774) were purchased from the American Type Culture Collection (ATCC, Rockville, MD).

The MDAH 2774 cell line was derived from the ascites fluid of a patient with endometroid ovarian carcinoma who had not received any chemotherapy or radiation prior the collection of cancer cells. They were originally characterized at the MD Anderson Hospital and Tumor Institute, Houston, TX and found to be hypotriploid (Freedman et al., 1978). Both cell lines were cultured in Eagle's Minimum Essential Medium (MEM; Gibco Labs, Grand Island, NY) supplemented with 10% heat inactivated fetal bovine serum (FBS; Gibco), 50 μg/ml gentamicin sulfate (Sigma Chemical Company, St. Louis, MO). All incubations, treatments and microtiter tetrazolium (MTT) assays were performed at 37 °C and with 5% CO_2 unless other conditions are stated.

2.2. Test solutions

Ascorbate sodium (Vitamin C or VC) and menadione bisulfite (VK_3) were purchased from Sigma Chemical Company. For the cytotoxicity experiments, the vitamins were dissolved in phosphate-buffered saline (PBS) to create 8000 μM VC, 500 μM VK_3 and 8000 μM VC:80 μM VK_3 test solutions. For the remainder of the studies, the vitamins were dissolved in culture medium to create test solutions with final concentrations of 2032 μM VC, 20.32 μM VK_3, 2032 μM VC:20.32 μM VK_3. In order to prevent photodegradation of the vitamins, vitamin solution preparation and all experiments were performed in a darkened laminar flow hood.

2.3. Cytotoxicity assay

The cytoxicity assay was performed using the microtetrazolium assay [MTT 3-(4,5-dimethylthiazol-2-yl)-2,5-diphenyl-diphenyltetrazolium bromide] assay as described previously (Venugopal et al., 1996b). Corning 96-well titer plates were seeded with tumor cells (5×10^3 per well) and incubated for 24 h. Vitamin test solutions were serially diluted with media in 12 two-fold dilutions. Each dilution was added to seven wells of the titer plates and co-incubated with the tumor cells for 3 days. After vitamin treatment and the incubation period, cytotoxicity was evaluated using the MTT assay. Following linear regression, the line of best fit was determined and the 50% cytotoxic dose (CD_{50}) was calculated. The fractional inhibitory concentration index (FIC) was employed to evaluate synergism. $FIC = CD_{50}^{A\,comb}/CD_{50}^{A\,alone} + CD_{50}^{B\,comb}/CD_{50}^{B\,alone}$, where $CD_{50}^{A\,alone}$ and $CD_{50}^{B\,alone}$ are 50% cytopathic doses of each vitamin alone; $CD_{50}^{A\,comb}$ and $CD_{50}^{B\,comb}$ are the 50% cytopathic doses of the vitamins administered together.

2.4. Cell culture

Titer dishes were seeded with 1.0×10^6 MADH cells, and the cells were allowed to attach and spread for 24 h at 37 °C. Following exposure of the MADH cell monolayers to each vitamin alone and in combination, cells were harvested at 1-, 2-, and 3 h intervals and processed for TEM observations, DNA histochemical staining and DNA extraction to study degradation.

2.5. Histochemistry

Circular coverslips were seeded with MDAH cells (1×10^5) and incubated for 24 h at 37 °C. The cells were then overlaid for 1-, 2-, and 3 h with media containing vitamins or with only media (Sham-treated group). All cells were washed twice with PBS, fixed for 1 h in formalin at room temperature and then washed three times for 5 min per wash with PBS. Feulgen DNA staining was achieved through a Schiff reaction according to the technique of de Tomasi (1936) using the 8 min hydrolysis time advised by Bauer in Pearse (1985) for the staining. No counterstain was used. After rinsing and dehydration in graded ethanol, the preparations were cleared in xylene before mounting in synthetic DPX medium. Control slides that were not hydrolyzed nor treated by Schiff after hydrolysis did not provide significant

staining of the chromosomes of dividing cells nor the DNA. All chemicals (at least 99% purity) were prepared and used from the same containers and originated from Fisher Scientific Co. (Pittsburgh, PA). Staining was accomplished simultaneously for all treated cells to avoid batch specific variations in DNA solubilization and Feulgen staining (Duijndam and Van Duijn, 1975). All dehydration and mountings were also made at the same time and in the same room conditions of light and temperature (17–18 °C). After a 2-h setting to allow polymerization of mounting medium, all sections were stored in the dark at 4 °C overnight and examined the next day. Micrographs were taken under immersion oil with an Olympus BX51 photomicroscope (Olympus America, Melville, NY). All micrographs were printed from Kodak Ektachrome 64T reversal film (Kodak, Eastman Kodak Co., Rochester, NY) and prints were made from slides by using same batch of paper and photographic reagents.

2.6. Densitometry of Feulgen staining

Densitometric measurements were obtained from all cell nuclei observed in the color micrographs printed from each treatment by using a X-Rite 820 transmission/reflexion densitometer (Grand Rapids, MI) at the same temperature and light intensity. Each of the nuclei reflectance intensity measurement was collected from several sets of illustrations printed per treatment (i.e. three series of 10 nuclei were measured per treatment). Data were computed after subtraction of the background intensity. Measurements of reflectance units were averaged in a histogram representation and presented with S.E.M. Despite the lack of a sophisticated cytophotometric system in our laboratory, this simple commercial equipment had an accuracy and stability allowing repeatable measurements within 1% of each reading.

2.7. Statistical analysis of Feulgen staining

Following a 1-h vitamin exposure, the possibility of enhanced DNA degradation with the VC:VK_3 combination was assessed by measuring decreases in the intensity of Feulgen staining of tumor DNA by reflectance densitometry and comparing these decreases to those obtained with either VC or VK_3 alone. A two-way ANOVA was used in which both vitamin treatments were crossed. The single-degree-of-freedom interaction test of the effect of the combination of VC and VK_3 followed directly from this two-factor model. Ten DNA densitometric measurements of MDAH cells were obtained within each of three independent sites on the microscopic preparations for each of the four conditions yielding 30 observations per experimental condition. The analysis of variance modeled the nesting of measurement within site (mixed modeling) so that there were three primary units of analysis (sites) for each condition. A significance level of 0.05 was used for the interaction test.

2.8. DNA gel electrophoresis

Five million MDAH 2774 cells and a similar number of MHRF human foreskin fibroblasts were plated and allowed to attach for 24 h. Cells were then exposed to the VC:VK_3 combination (2032 μM VC:20.32 μM VK_3) for 4 h, washed with PBS and scraped from the titer dishes. After centrifugation at 1000 × *g*, the supernatant was discarded. The cell pellets were resuspended in 0.4 ml digestion buffer (100 mM NaCl, 10 mM Tris–HCl pH 8.0, 25 mM EDTA, 0.5% SDS, 0.1 mg/ml proteinase K). Proteins were removed by extractions with an equal volume of 50% equilibrated phenol, 48% chloroform, 2% isoamyl alcohol (PCIA). Samples were vortexed for 30 s, then centrifuged for 5 min at 16,000 × *g* in a microcentrifuge. The aqueous phase was re-extracted with equal volumes of PCIA until the interface between the organic and aqueous phases was transparent. Nucleic acids were then precipitated from solution by adding sodium acetate pH 5.2 to a final concentration of 0.3 M and 1.5 vol. of ethanol. Samples were centrifuged for 15 min at 16,000 × *g* in a microcentrifuge, supernatant discarded and excess salts removed by washing the pellet with cold 75% ethanol. Pellets were dried, suspended again in 40 μl of 10 mM Tris–HCl pH 8.0, 1 mM EDTA and 2 μl of 10 mg/ml RNase A. Five microliters of the resulting preparation, representing DNA from 6×10^5 cells, was run on a 0.6% agarose gel in 0.089 M Tris-borate, 0.089 M boric acid, 0.002 M EDTA (Sambrook et al., 1989), at 1 V/cm for 18 h. The gel was then stained with ethidium bromide and analyzed by a Kodak Electrophoresis and Documentation System 120 (Eastman Kodak Co., Rochester, NY).

2.9. For TEM

MADH cells cultivated in flasks were allowed to grow as a monolayer and exposed either to VC alone, VK_3 alone or VC:VK_3 combination for 1 h. Cells were washed in PBS buffer, harvested and allow to sediment by slow centrifugation (450–500 rpm). After removal of the supernatant, cells were fixed in 2.5% phosphate-buffered glutaraldehyde solution (with 0.13 M sucrose-phosphate, pH 7.35, modified Karnovsky method, 1967) for 30 min at room temperature in 2 mm^3 microfuge tubes. After two 10-min washes in sucrose-phosphate buffer and gentle sedimentation of a formed pellet of cells for each treatment, a 30-min postfixation was in aqueous 1% osmium tetroxide solution, under a fume hood, and at room temperature. Pellets, now contrasted by this postfixation, were washed twice for 10 min in the same buffered solution before dehydration and processing into PolyBed epoxy resin (Polysciences, Warrington, PA). One-micrometer thick sections were then stained in toluidine blue to select areas for ultramicrotomy. These sections were collected on 75- and 100-mesh hexagonal copper grids (SPI, West Chester, PA), stained in uranyl acetate and lead citrate, and examined in a Zeiss EM-10 TEM (Carl Zeiss, Thornwood, NY). The digitized images

were obtained using an analySIS 2.1 software system© (Soft Imaging System GmbH, Lakewood, CO and Münster, Germany) in the Pathology Department of the Childrens' Hospital Medical Center of Akron, OH.

3. Results

3.1. Antiproliferative activity of the vitamins

Table 1 illustrates that vitamin treatment of the MDAH cells resulted in a CD_{50} value of 1528 μM for Vitamin C, 41.8 μM for Vitamin K_3 and 165 μM:1.65 μM for the VC:VK_3 combination. These results represent a nine-fold decrease of the CD_{50} of Vitamin C and a 25-fold decrease for Vitamin K_3. Vitamin treatment of MHRF cells resulted in a CD_{50} value of 8000 μM for Vitamin C, 500 μM for Vitamin K_3 and 1000 μM:10.0 μM for the VC:VK_3 combination. These results represent a eight-fold decrease of the CD_{50} of Vitamin C and a 50-fold decrease for Vitamin K_3. The CD_{50} value of the vitamin combination for the MHRF fibroblasts is six-fold greater than CD_{50} value of the vitamin combination for the MDAH cells (i.e. 1000 μM/165 μM). The fractional inhibitory concentration index (FIC) has been used to evaluate the synergism of the vitamins. While an FIC < 1.0 indicates that the combination is synergistic, an FIC > 1.0 indicates the combination is antagonistic. An FIC $= 1.0$ indicates the combination is indifferent. The FIC for MDAH cells is 0.147, which is indicative of a synergistic interaction of the vitamins. The FIC for MHRF cells is 0.145, which is also indicative of a synergistic interaction of the vitamins.

3.2. Light microscopic DNA observations

Fig. 1 illustrates representative micrographs of Sham-treated (CONT) and vitamin treated MDAH cells whose nuclei have been stained according to the Feulgen technique for relative DNA content. The rows of mounted micrographs display changes in Feulgen staining patterns following 1, 2 and 3 h treatment (columns) with culture medium (CONT), VC alone, VK_3 alone or with the VC:VK_3 combination.

At all three time points, Feulgen stained CONT cells are uniformly contrasted. These cells display ovoid magenta nuclei surrounded by pale-lilac cytoplasms that are non-specifically stained by the Schiff base during dehydration of the cells. The abundant cytoplasm of the control cells enables one to see the multipolar shape of most of the MDAH cells. These cells are superimposed on top of each other that is indicative of the absence of contact inhibition. In some favorable cases when the control cells are viewed through immersion oil, many elongated, particulate structures that are probably mitochondria are visible.

Following VC treatment, MDAH cells show a lesser degree of nuclear staining than control cells which is indicative of diminished DNA content. After 1 h VC-treatment, well-stained marginated chromatin and large, oblong, poorly stained, nucleolar masses are visible. Following 2 h VC treatment, many cells are smaller than in control cells owing to a reduction in the cytoplasm. However, a small number of cells with large diameters and very large nuclei can also be seen. After 3 h VC treatment, all nuclei are smaller than control nuclei and the population of cells attached to the coverslips is less numerous than for the 1 h- and 2 h-VC treatments. Exposure of the MDAH cells to VC resulted in two populations of cells: those undergoing autoschizis and those that have been blocked at G_1/S in the cell cycle. By 3 h VC treatment, many of the cells undergoing autoschizis have detached from the coverslip leaving those that are blocked. These blocked cells exhibit far less derangement than the autoschizic cells (Von Gruenigen et al., 2003).

After VK_3 treatment, the nuclei are more intensely stained than was the case following 1 h-VC treatment (see average reflectance in Fig. 2B). While the nuclei of the 1 and 2 h VK_3-treatment groups are still well stained, cell size is reduced by the loss of cytoplasm via autoschizic excisions (see in Fig. 1 VK_3 1 h and inserts). Some of these cells display asymmetrical cytokinesis and clear-cut dotted margination of chromatin (Fig. 1, VK_3 1 h, top insert). After 2 h-VK_3 treatment, most cells appear smaller than both the control cells and VC-treated cells due the excision of cytoplasmic pieces. Many of these cells exhibit marginated chromatin with a reticulated pattern (Fig. 1 VK_3 2 h). The large, pale, ovoid masses in these nuclei are the segregated nucleolar ribonucleoproteins that are surrounded by blocks of DNA-containing chromatin. Finally, after 3 h of VK_3 treatment, small MDAH cells are detected and consist of poorly stained nuclei surrounded by well-delineated but narrow rims of cytoplasm.

After treatment with the VC:VK_3 combination, MDAH cells exhibit a variety of cell shapes. A time dependent re-

Table 1
Antitumor activity of vitamins

Cell line	Vitamins alone		Vitamins together		Fractional inhibitory concentration (FIC)
	Vitamin C 50% cytotoxic dose (μM)	Vitamin K_3 50% cytotoxic dose (μM)	Vitamin C 50% cytotoxic dose (μM)	Vitamin K_3 50% cytotoxic dose (μM)	
MDAH	1528 ± 29	41.8 ± 0.62	165 ± 1.5	1.65 ± 1.53	0.147
MRHF	8000 ± 246	500 ± 5.0	1000 ± 28	10 ± 0.2	0.145

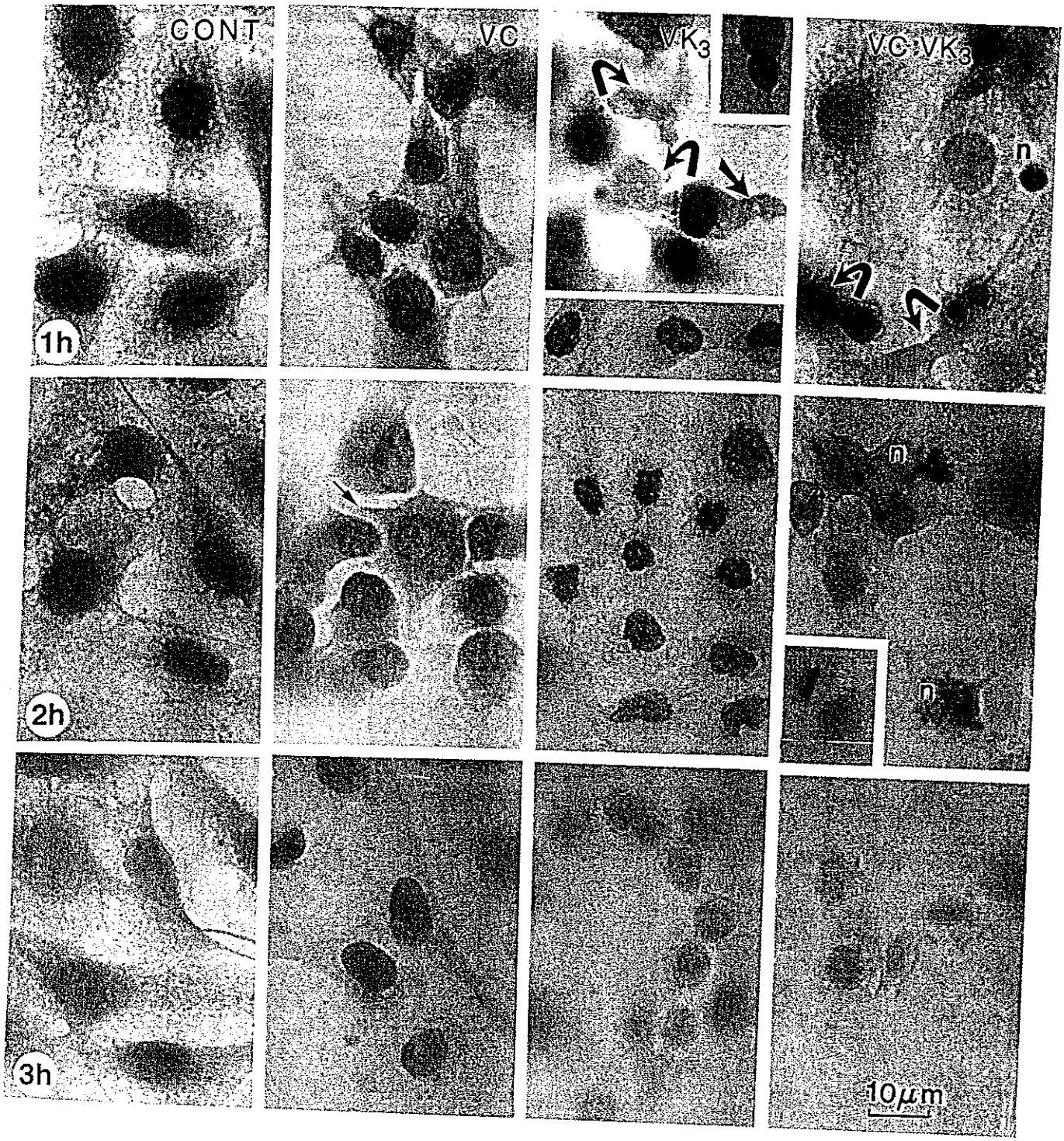

Fig. 1. A color photomontage illustrates the Feulgen staining of the DNA of human ovarian carcinoma (MDAH 2774) cells. The treatment regimen (Sham-treated (CONT), ascorbate (VC), menadione alone (VK_3) or the vitamin combination ($VC:VK_3$)) is indicated on top of each column. The rows correspond to exposure time (1-h (1h), 2-h (2h), and 3-h (3h)). Selected nuclei are denoted as "n". Small arrows indicate fluidic membrane extensions while curved and straight arrows denote the self-excisions of cytoplasm. In $VC:VK_3$-treated cells, extranuclear DNA can be seen in autophagosomes. The scale is 10 μm in all micrographs.

duction in number of adherent cells and staining contrast for chromatin is also apparent. After 1 h of treatment (Fig. 1, $VC:VK_3$ 1 h), the ongoing self-excisions and the progressive reduction of cell size that characterizes autoschizis are evident. One can notice a few cells reduced to nuclei surrounded by narrow rims of cytoplasm. After 2 h-$VC:VK_3$ treatment, most of the remaining cells are reduced in size and appear clustered in small groups. The nuclei of these cells are stained a pale lilac color, demonstrating a significant loss of DNA. Some Feulgen-stained material is located in the

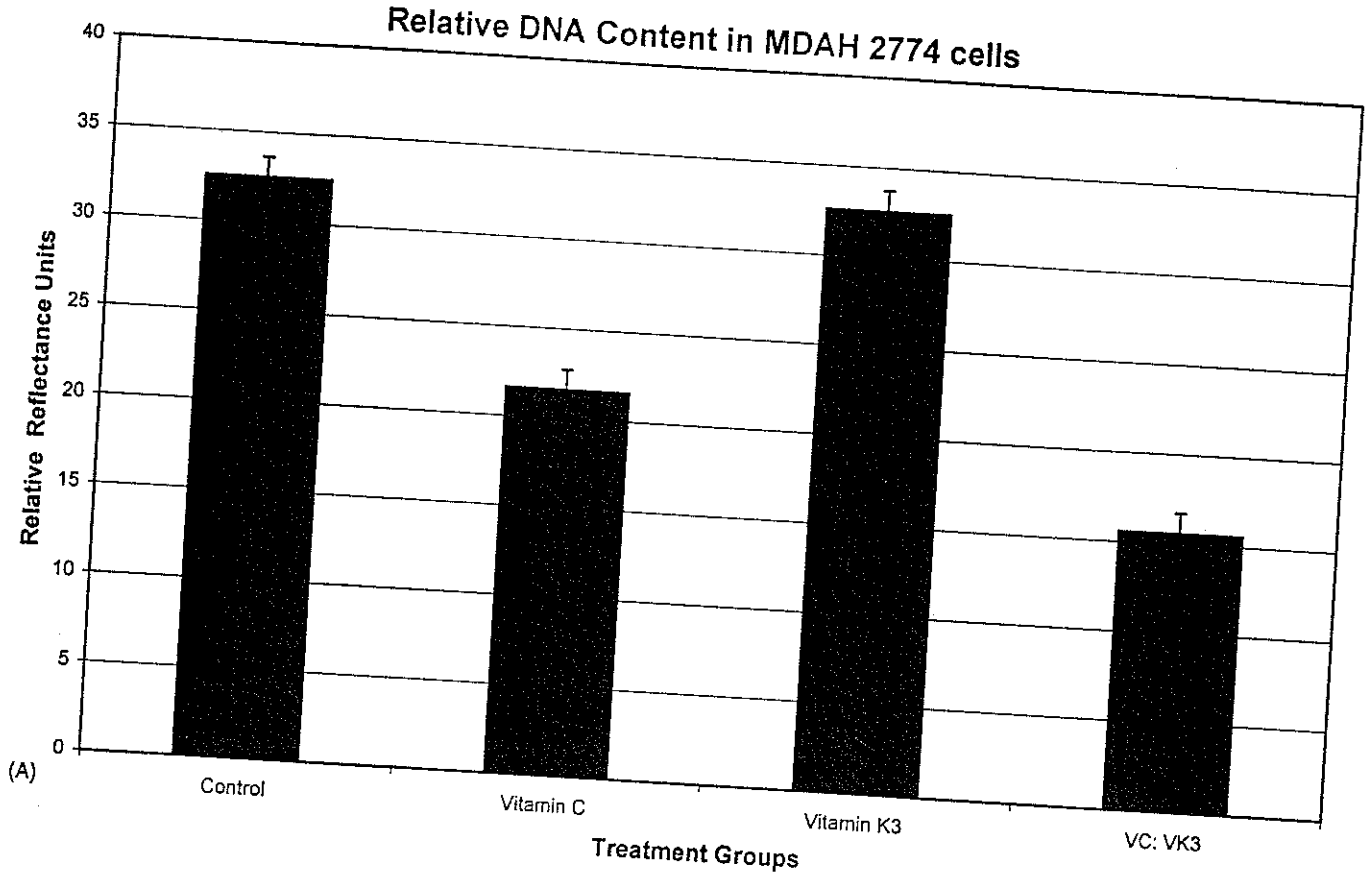

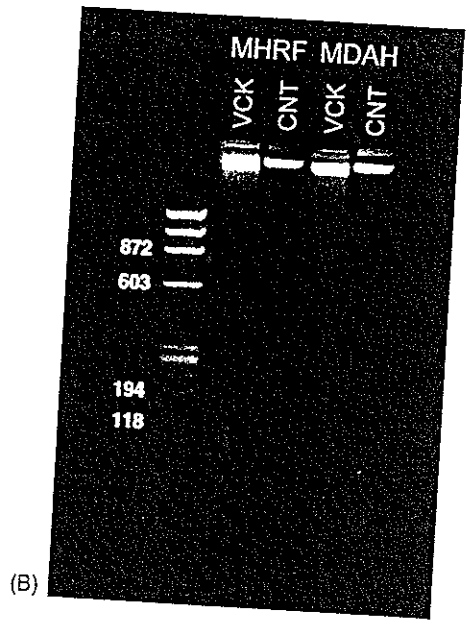

Fig. 2. (A) This histogram summarizes the relative DNA content of control and vitamin treated MDAH 2774 cells. The bars represent densitometric measurements of the intensity of reflectance from the color illustrations in Fig. 1 minus the background reflectance. (B) Gel electrophoresis of the total DNA extracted from sham treated and VC:VK_3 treated human foreskin fibroblasts (MHRF) and MDAH 2774 cells. Lane 1 contains a molecular weight marker. Lane 2 contains the DNA from VC:VK_3 treated MHRF cells (VCK), while lane 3 contains the DNA from sham-treated MHRF cells (CNT). Lane 4 contains DNA from vitamin treated MDAH cells (VCK), while lane 5 contains DNA from sham treated MDAH cells (CNT).

cytoplasm that surrounds these poorly stained nuclei. The inset of Fig. 1 VC:VK_3 2 h demonstrates intensely Feulgen stained clumps of DNA among the unstained cytoplasm of an MDAH cell that is undergoing autoschizis. This DNA degradation and autoschizis is increased in the 3 h treatment group where minute cells are seen to be undergoing further cytoplasmic self-excisions as well as nuclear diminution and degradation. In this treatment group, the nuclear mass is detectable as a poorly stained, pinkish chromatic material.

3.3. Densitometric measurements

Measurements of the DNA in nuclei of MDAH cells were made only after a 1-h vitamin exposure due to the abundance of cell death, detachment and disintegration for longer vitamin exposures. In Fig. 2A, the DNA staining intensity of sham-treated (Control cells) is 32.5 ± 1.127. The DNA staining intensity values for VC and VK_3 alone are 21.6 ± 1.127 and 32.6 ± 1.127, while the DNA staining intensity of the vitamin combination is 15.6 ± 1.127. Notice that the average DNA level following VK_3 is the same as in the control group. By contrast, the DNA level following VC or VC:VK_3 treatment is significantly lower than in the control group ($P < 0.0001$). In addition the DNA intensity level following VC:VK_3 treatment is significantly different from the DNA intensity level following VC treatment ($P < 0.03$). The standard error values are all identical because they were based on a pooled variance estimate.

3.4. DNA gel electrophoresis

In an effort to confirm that DNA was cleaved during VC:VK_3 treatment, total DNA was extracted from MDAH cells and MHRF human foreskin fibroblasts following sham treatment or 4 h treatment with the vitamin combination. The DNA was then resolved electrophoretically as shown in Fig. 2B. Lanes 2 and 3 contain the DNA of VC:VK_3-treated (VCK) and sham-treated (CNT) MHRF cells. The DNA from the sham-treated MHRF cells appears as a single high molecular weight band slightly below the well in which it was loaded. Conversely, the DNA from VC:VK_3 treated MHRF cells appears as a low molecular weight smear at or below 200 bases. The DNA from sham-treated MDAH cells also appears as a single high molecular weight band slightly below the well in which it was loaded, while the DNA from vitamin treated MDAH cells exhibits a spread pattern. The absence of laddering in the vitamin-treated lanes strongly suggests that VC:VK_3-induced cell death is not apoptosis.

3.5. Transmission electron microscopy

The sham-treated MDAH 2774 cells are round and poorly differentiated with diameters between 15 and 35 μm. Short microvilli-like filopodia (1–1.5 μm long) extend from the cells and sometimes bifurcated. Most of the cytoplasm appears relatively electron dense owing to fine ribonucleoprotein granules, while the peripheral cytoplasm contains numerous glycogen-like particles. A few fat-containing vacuoles can be detected by the presence of a residual, osmiophilic content. A large number of rough and smooth endoplasmic cisternae are distributed throughout the remaining cytoplasm. The large nuclei appear ovoid or deeply indented by a deep, narrow groove. Because of its large size, only the edge of the intranuclear branching structure of the nucleolus is often detected (Fig. 3). The overall nucleoplasm is euchromatic with the delicate thickening of the inner nuclear membrane being clearly interrupted by nuclear pores.

After a 1 h VC treatment (Fig. 4), the cells remain spherical and are covered by numerous, long, slender microvilli or filopodia. The largest, rounded cells display vacuolated blisters ($d < 1$ μm) and blebs. Following a 2 or 3 h VC treatment, these cells often show larger cytoplasmic defects (Fig. 1 VC 2 or 3 h), while nuclei appear more spherical and eventually show a discrete concavity. The nuclear chromatin becomes patchier and forms condensates which thicken the inner nuclear membrane without obstructing the nuclear pores (Fig. 5). Moreover, the nucleolar-associated chromatin has segregated outside the nucleolus in a circumferential ring while the granular component appears as a compact, electron-dense mass associated with a depression of the nuclear envelope. The overall nucleoplasm appears finely mottled with frothy vesicles and is suggestive of a future karyorrhexis.

Following VK_3 treatment, the cells are pleiomorphic. While 1–1.5% of the cells are multinucleate, the majority of the cells are uninucleate and appear either subspherical with fusiform to elongate regions or spindle-shaped (Fig. 5). Pieces of cytoplasm ($d = 1.5$–5 μm) and blisters of varying size are in the process of being excised. Unlike apoptosis, these cytoplasmic fragments do not contain any detectable membranous organelles or any nuclear fragments (such as apoptotic bodies). As a consequence of these progressive self-excisions, cells diminish their size by more than one third and leave organelles clustered around the nuclei in a thin rim of cytoplasm.

Figs. 3–9 depict progressive nucleoplasmic alterations that result from changes in the chromatin. The majority of the cells exhibit well contrasted chromatin which decorates the inner nuclear envelope in a layer 0.2–0.5 μm thick and remains associated with and penetrates a huge, round nucleolus.

Subsequently, these chromatic bodies become more eccentrically located and appear only as electron dense patches along the nuclear envelope (Fig. 5). The final stage in the process (Fig. 6) before karyorrhexis and karyolysis is the swelling of the remaining organelles and nuclear envelope.

Following VC:VK_3 treatment, alterations in cell ultrastructure are a composite of those seen during individual vitamin administration and are observed in virtually every cell.

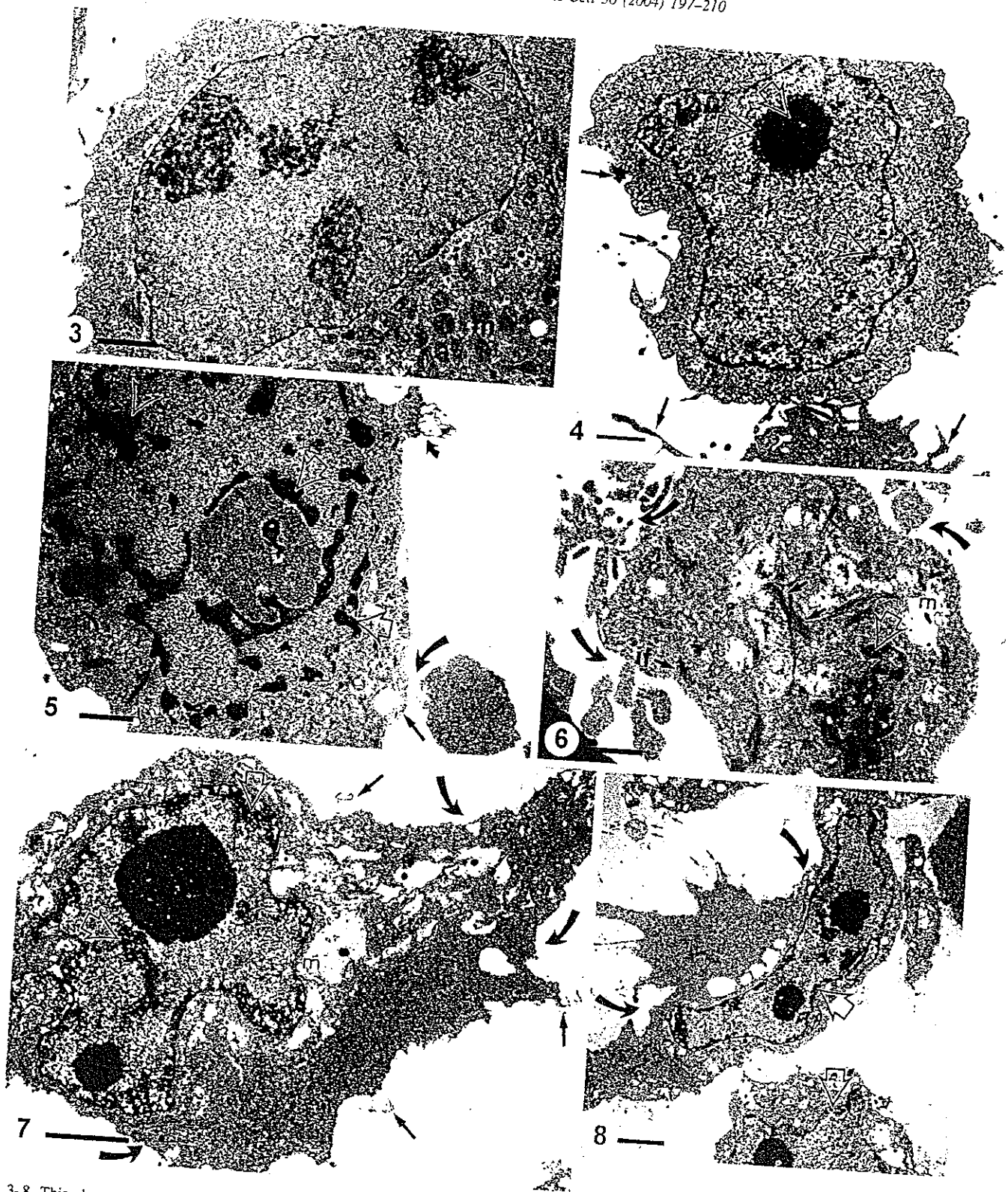

Figs. 3–8. This photomontage illustrates TEM views of nucleus and perinuclear areas of human ovarian MDAH 2774 carcinoma cells before (Fig. 3) and after 1 h treatment (Figs. 4–8). All the scales equal 1 μm. (Fig. 3.) A sham-treated cell contains a large indented nucleus with a branching nucleolus with several fibrillar centers (clear arrow) and small mitochondria (m). (Fig. 4.) Vitamin C-treated cells display blebs and long microvilli (arrows) and possess a round nucleolus with one large fibrillar center and a narrow rim of associated chromatin (open arrows). (Fig. 5.) Following Vitamin K_3 treatment, cells contain a compact nucleolus. Patches of chromatin (open arrows) are distributed in the outer portion of the nucleoplasm. Peripheral cytoplasmic defects (arrows), large cytoplasmic blisters and self-excisions (small curved arrow) are also visible. (Figs. 6–8.) Following 1 h VC:VK_3 treatment, the cells are of significantly smaller than in all the other treatments. Mitochondrial remnants (m) are detected in the peripheral cytoplasm. Disorganized intermediate filaments (if) can be seen alongside many blisters (small arrows) and cytoplasmic self-excisions devoid of membranous organelles (curved arrows). Ribonucleoproteinaceous masses appear as a scalloped outline of the inner nuclear envelope (clear arrows).

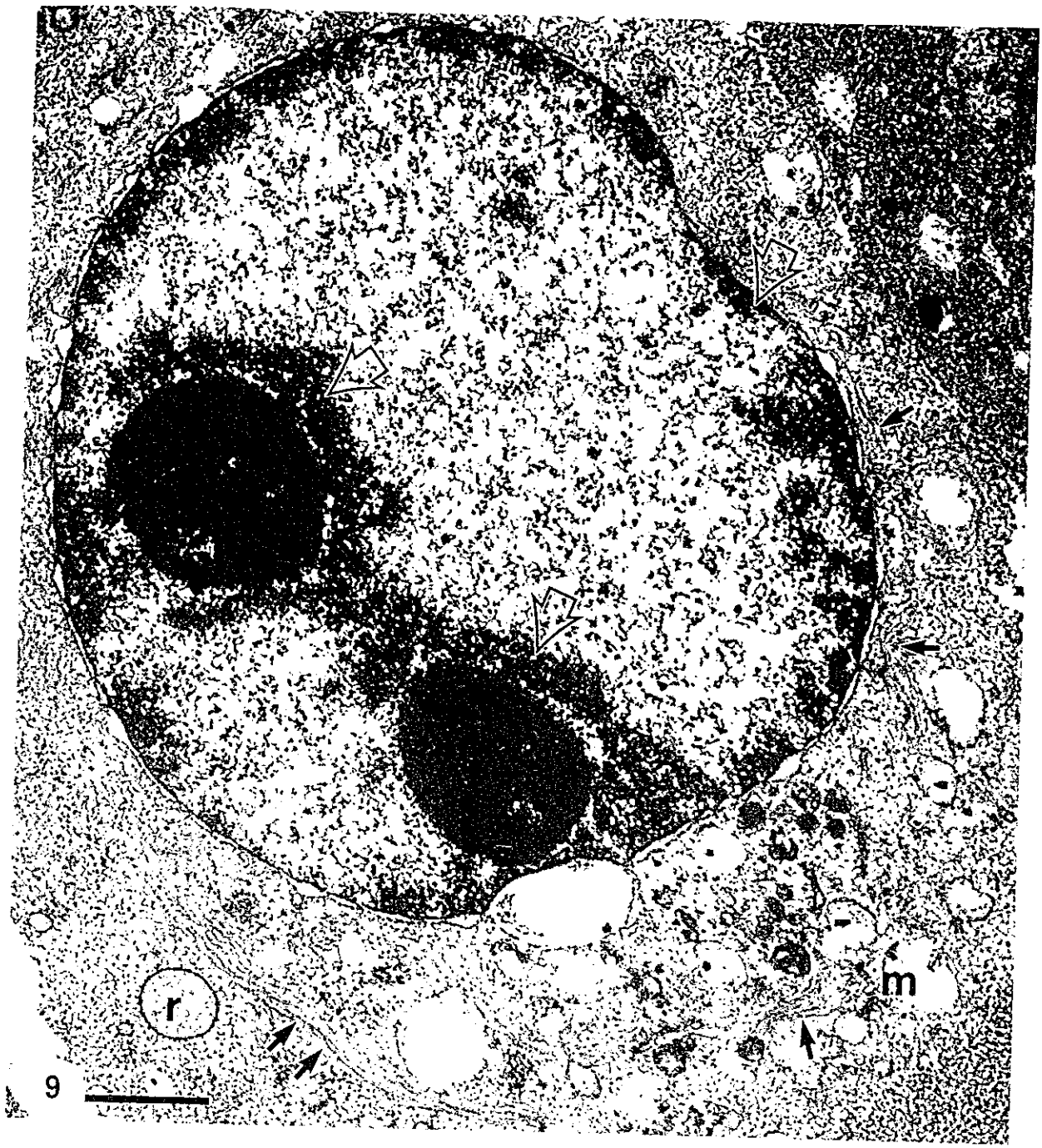

Fig. 9. An enlarged TEM view of one MDAH ovarian carcinoma cell after 1 h VC:VK_3 treatment shows a segregated nucleolus as two compact masses covered by chromatin (clear arrows). Swollen mitochondria (m) dilated rough ER (r) pieces and strings of intermediate filaments (small arrows) surround the nucleus. Scale equals 1 μm.

However, the alterations are exacerbated and occur more rapidly (1 h versus 3 h) than with individual vitamin treatment (Figs. 6–9). In addition to these changes, the majority of mitochondria exhibit condensed bodies in their matrices while their inner and outer membranes apparently remain intact. The intermediate filaments of the cytoskeleton appear in bundles surrounding the nucleus and the organelles. Finally, the rough endoplasmic reticulum, first to degranulate in case of cell injury, is maintained intact until near the completion of autoschizis (Fig. 9).

4. Discussion

4.1. Cancer cells and enzyme activities against reactive oxygen species (ROS)

Tumor cells contain 10- to 100-fold lower catalase activity than normal cells (Benade et al., 1969; Keller et al., 1993). Similarly, cancer cells have been shown to have little or no mitochondrial superoxide dismutase activity (Dionisi et al., 1975). This relative absence of free radical detoxi-

fying enzymes in tumor cells suggests that these cells may be more susceptible to the cytotoxic effects of ROS than non-tumor cells.

4.2. The antiproliferative activity of ascorbate (VC) treatment

VC has been shown to inhibit cancer cell growth in vitro (Benade et al., 1969; Yamafuji et al., 1971; Leung et al., 1993; Gilloteaux et al., 1998a, 2001b) and in vivo (Varga and Airoldi, 1983; Taper et al., 2001, etc). VC also specifically kills tumor cells (Benade et al., 1969; Bram and Fridovich, 1981; Leung et al., 1993; Sakagami and Satoh, 1997). Because of its tumor specific cytotoxicity, it has been suggested that VC alone or in conjunction with traditional chemotherapeutic regimens may prolong the life of cancer patients (Yamafuji et al., 1971; Cameron and Pauling, 1976; Cameron et al., 1979; Tsao et al., 1988; Taper et al., 1987, 1996, 2001; Riordan et al., 1995; Gilloteaux et al., 2001b; Jamison et al., 2001).

VC in the form of ascorbate preferentially accumulates and is metabolized as ascorbate salts by cancer cells (Sakagami and Satoh, 1997). Once inside the cell, VC can be oxidized either by single- or two-electron transfer and can be converted back to ascorbate by NADH-dependent semihydroascorbate reductase or glutathione-dependent dehydroascorbate reductase (Koch and Biaglow, 1978; De Laurenzi et al., 1995). This cycling process creates intracellular H_2O_2 and other ROS that deplete cellular thiol levels, initiate membrane lipid peroxidation and leads to the rapid elevation of intracellular calcium levels (Farber, 1982; Farber et al., 1990; Sakagami and Satoh, 1997). In the presence of iron or catalase inhibitors, these VC-induced peroxidations increase dramatically (Benade et al., 1969; Chakraborty et al., 2001). The peroxidative action of VC-induced ROS on cell membranes (Taper et al., 1987; Lupulescu, 1992; De Laurenzi et al., 1995) is observed in some metabolic changes (Venugopal et al., 1996a,b), and as blister and bleb formation, decreased membrane viscosity (Gilloteaux et al., 1998a,b,c,d, 1999, 2001a,b,c); or mitochondrial damage (Gilloteaux et al., 1995; Jamison et al., 1997). Once cellular membrane integrity is compromised, free calcium level rises in the cancer cell and interferes with mitochondrial function or prevents the high output of ATP necessary to repair and/or maintain cell homeostasis. Another consequence of elevated calcium levels may be the activation of DNase II which in conjunction with ROS may inhibit DNA synthesis, alter nucleosides and induce DNA strand breaks (Ishida and Takahashi, 1975; Morgan et al., 1976; Lesko et al., 1980; Bram and Fridovich, 1981; Lupulescu, 1991).

4.3. The antiproliferative activity of menadione treatment

VK_3 is a synthetic derivative of Vitamin K_1, it exhibits antiproliferative activity against liver, cervix, nasopharynx, colon, lung, stomach, breast, leukemia and lymphoma cell lines (Prasad et al., 1979; Nutter et al., 1991; Wu et al. 1993a,b). At least a portion of this antiproliferative activity may be due to the ability of VK_3 to induce cell cycle arrest or delay at both the G_1/S and G_2/M phases of the cell cycle (Wu et al., 1993a,b; Jamison et al., 1996, 2004). However, VK_3 has also been shown to be cytotoxic to a variety of urological tumors with another mechanism of action being responsible for the cytotoxicity (Venugopal et al., 1996a,b; Ervin et al., 1998; Gilloteaux et al., 1998a,b,c,d, 1999, 2001a,b,c,d; Taper et al., 2001). VK_3 can be reduced intracellularly via one- to two-electron transfer to form a semiquinone or hydroquinone that can be converted back to the quinone by a variety of cellular enzymes. This redox cycling leads to the generation of superoxide and more toxic ROS via metal-catalyzed reactions (Venugopal et al., 1996a,b, 1997; Jamison et al., 2001, 2002). Consequently, VK_3 is a strong oxidative substance (Begleiter, 1983) that induces a complex cytotoxic stress response (Caricchio et al., 1999) and the drastic reduction in cellular glutathione and NADPH pools (Carbonera and Azzone, 1988).

This oxidative stress also manifests itself in striking changes in cellular architecture due to the oxidation of the SH groups of actin and other actin regulatory proteins, intermediate filaments, lamins and keratin (Sanger and Sanger, 1983; Hinshaw et al., 1986; Yang et al., 1994; Maraldi et al., 1998; Minamitsuji-Mochizuki et al., 1999). Consequently, the cells acquire an elongate to fusiform shape and shed small and large cytoplasmic fragments (Bellomo et al., 1990; Malorni et al., 1991; Wu et al., 1993a,b). Mitochondrial and nuclear architecture is also disrupted (Wu et al., 1993a,b; Jamison et al., 1997; Gilloteaux et al., 2001d). Complementary to these effects, VK_3 has been shown to damage DNA (Ngo et al., 1991) and to reactivate DNase I activity in tumor cells where DNase I is known to be inhibited (Taper et al., 2001).

4.4. The antiproliferative activity of the VC:VK_3 combination

The vitamin combination has been shown to exhibit synergistic in vitro antiproliferative activity against liver, endometrial, oral epidermoid, breast and a wide variety of human urologic tumor cell lines as well as in vivo antiproliferative activity against liver and prostate cancer (Taper et al., 1987; Jamison et al., 2001). At least a portion of this antiproliferative activity may be due to cell cycle arrest at G_1/S and G_2/M (Jamison et al., 1996, 2004). Additional antiproliferative activity may be cytotoxicity related to an increased rate of redox cycling and ROS production due to the ability of VC to facilitate the single electron cycling of VK_3 (Jarabak and Jarabak, 1995; Pething et al., 1983). Because of the redox cycling and ROS production of the vitamin combination, the homeostasis of the MDAH cells is more rapidly disturbed and the cytological insults are greater than with either vitamin alone.

Finally, the spread DNA pattern following electrophoresis (Fig. 2B) suggests that DNA degradation was not part of an apoptotic process. While these results are consistent with the sequential reactivation of both DNase I and II (Taper et al., 1987, 2001), they do not preclude the possibility that the decreased Feulgen staining may be related to ROS-induced DNA damage stemming from an increased rate of redox cycling. Therefore, additional experiments must be performed to unequivocally determine the mechanism responsible for this DNA degradation.

In previous in vivo studies, sub-therapeutic doses of VC and VK_3 were administered to the test animals so that the vitamins only exerted their cytotoxic effects when both vitamins were present together in the tumor cells. Under these conditions, selective and sequential reactivation of DNase I by VK_3 and DNase II by VC in the vitamin combination, resulted in synergistic degradation of DNA and tumor regression (Taper et al., 1987, 2001). To simulate these conditions in vitro and to ensure that we did not miss the window of activity and synergism, the vitamins were administered at concentrations where one vitamin alone (VC) was active, while the other vitamin (VK_3) was only marginally active. MTT cytotoxicity assays with the vitamins produced CD_{50} values of 1528 μM for Vitamin C, 41.8 μM for Vitamin K_3 and 165 μM/1.65 μM for the VC:VK_3 combination. Therefore, the dose of VC used in the current study (2032 μM) was slightly greater than CD_{50} value of 1528 μM. To maintain VC:VK_3 ratio of 100:1, 20.32 μM VK_3 was used. Since the CD_{50} of VK_3 is 41.8 μM and the dose of VK_3 employed in this study is 20.32 μM, the activity of the VK_3 is expected to be much less than the activity of the VC. Indeed, VC treatment produces a significant decrease in Feulgen staining of DNA, while VK_3 treatment has little effect on Feulgen staining. However, when VK_3 is administered with VC, there is an additional significant decrease in Feulgen staining of DNA beyond what is observed for VC alone.

4.5. Specificity of the antiproliferative and antitumor response of the VC:VK_3 combination

The results of this study demonstrated that the CD_{50} value of the vitamin combination for the MHRF fibroblasts is six-fold greater than CD_{50} value of the vitamin combination for the MDAH cells. These results agree with those of Zhang et al. (2001) who showed that while VC and VK_3 induced synergistic cytotoxicity against fibroblasts as well as tumor cells, fibroblasts were not as sensitive to the cytotoxic effects of the vitamins as the tumor cells. In addition, in the current study, the FIC values for the MDAH cells and the MHRF cells are nearly identical (0.147 versus 0.145). These results suggest that once cytotoxic doses are reached in non-tumor cells, the vitamins exhibit the same type of synergistic toxicity observed in tumor cells. Since the CD_{50} value for VC:VK_3 treated MHRF cells is 1000 μM:10.0 μM and the vitamins were administered at a dose of 2032 μM:20.32 μM, one would expect to see some cytotoxicity in the fibroblasts. In fact, a low molecular weight smear is seen in Fig. 2B when total DNA of MHRF cells is examined.

These in vitro results suggest a very narrow therapeutic window for the vitamin combination. However, the results of in vivo studies demonstrated that administration of clinically attainable doses of oral vitamins could significantly reduce the growth rate of solid prostate cancer tumors in nude mice without any significant bone marrow toxicity, changes in organ weight or pathological changes of these organs (Jamison et al., 2001). Likewise, no toxicity was observed when immunocompetent mice were given the vitamin combination daily at the same dose as described previously for 1 year (Ricchiuti et al., 2003).

4.6. Autoschizis, a new form of cell death, and histochemical changes suggests a potentially important ovarian cancer treatment

Several trends are evident from this study. First, there is a significant decrease in the viable adherent cell population in the sequence Sham-Control > VC > VK_3 > VC:VK_3. Second, cell diameters decrease from 15–35 to 7–12 μm in the same sequence. Third, extreme pleiomorphism, cell damage, and progressive self-morsellation results from vitamin treatment in the order VC:VK_3 > VK_3 > VC > Sham-Control. Ultrastructural damages appear to correlate at least qualitatively with decreases in Feulgen staining (DNA content), self-morsellation and DNA damage in the sequence VC:VK_3 > VC > VK_3 > Sham-Control. Fourth, plasma membrane and intracellular membrane damage, extreme mitochondrial defects, including swelling and some cytoskeletal defects increase following vitamin treatment in the sequence VC:VK_3 > VC > VK_3 > Sham-Control. Fifth, progressive nuclear changes (from redistribution of euchromatin producing a thin margin of DNA along the nuclear envelope and dissolution) and nucleolar changes (from branching to compaction, segregation and crystallization of the ribonucleoproteins into a single round body) are seen following vitamin administration in the sequence VC:VK_3 > VC > VK_3 > Sham-Control. These processes contribute to cell death by autoschizis (Gilloteaux et al., 1995, 1998a,b, 2001a,b,c,d, 2003a,b; Jamison et al., 1996, 2001, 2002, 2004; Venugopal et al., 1996a,b; Ervin et al., 1998). In addition, the results of two other studies indicate that VC:VK_3 autoschizis in MDAH cells is more frequent than apoptosis or oncotic necrosis (Gilloteaux et al., 2003a,b).

Acknowledgements

This report is dedicated to the late Lonnie Russell, Ph.D., the former editor of this journal. The authors would like to thank Dr. Brian Eyden, Christie Hospital NHS Trust, Manchester, UK for his review and constructive critiques of

the manuscript. Mrs. V. Androulakakis, Office of Biostatistics, NEOU College of Medicine, is thanked for her assistance provided in testing the data collected to support this manuscript and Ms. Th. Moles is recognized for the excellent TEM technical assistance provided at the Children's Hospital Medical Center of Akron, Ohio. This study was supported by Summa Research Foundation, Akron Ohio and by grant 97B048 from the American Institute for Cancer Research, Washington, DC.

References

Begleiter, A., 1983. Cytocidal action of the quinone group and its relationship to antitumor activity. Cancer Res. 43, 481–484.

Bellomo, G., Mirabelli, F., Vairetti, M., Iosi, F., Mallorni, W., 1990. Cytoskeleton as a target in menadione-induced oxidative stress in cultured mammalian cells: biochemical and immunocytochemical features. J. Cell Physiol. 143, 118–128.

Benade, L., Howard, T., Burk, D., 1969. Synergistic killing of Ehrlich ascites carcinoma cells by ascorbate and 3-amino-2,3,4-triazole. Oncology 23, 33–43.

Bram, K., Fridovich, I., 1981. DNA strand scission by enzymatically generated oxygen radicals. Arch. Biochem. Biophys. 206, 414–419.

Calderon, P.B., Cadrobbi, J., Marques, C., Hong-Ngoc, N., Jamison, J.M., Gilloteaux, J., Summers, J.L., Taper, H.S., 2002. Potential therapeutic application of the association of Vitamins C and K3 in cancer treatment. Curr. Med. Chem. 9, 2271–2285.

Cameron, E., Pauling, L., 1976. Supplemental ascorbate in the supportive treatment of cancer: reevaluation prolongation of survival times in terminal human cancer. Proc. Natl. Acad. Sci. U.S.A. 75, 4538–4542.

Cameron, E., Pauling, L., Leibovitz, B., 1979. Ascorbic acid and cancer: a review. Cancer Res. 39, 663–681.

Carbonera, D., Azzone, G.F., 1988. Permeability of inner mitochondrial membrane and oxidative stress. Biochim. Biophys. Acta 943, 245–255.

Caricchio, R., Kovalenko, D., Kaufmann, W.K., Cohen, P.L., 1999. Apoptosis provoked by the oxidative stress inducer menadione (Vitamin K_3) is mediated by the Fas/Fas ligand system. Clin. Immunol. 93, 65–74.

Chakraborty, H., Ray, S.N., Chakrabarti, S., 2001. Lipid peroxidation associated protein damage in rat brain crude synaptosomal fraction mediated by iron and ascorbate. Neurochem. Int. 39, 311–317.

Daoust, R., Amano, H., 1963. Ribonuclease and deoxyribonuclase activities in experimental and human tumors by histochemical substrate film method. Cancer Res. 23, 131–134.

De Laurenzi, V., Melino, G., Savini, I., Annicchiarico-Petruzelli, M., Finazi-Agro, A., Avigliano, L., 1995. Cell death by oxidative stress and ascorbic acid regeneration in human neuroectodermal cell lines. Eur. J. Cancer 31A, 463–466.

De Loecker, W., Janssens, J., Bonte, J., Taper, H.S., 1993. Effects of sodium ascorbate (Vitamin C) and 2-methyl-1,4-naphtoquinone (Vitamin K_3) treatment on human tumor cell growth in vitro. II. Synergism with combined chemotherapy action. Anticancer Res. 13, 103–106.

de Tomasi, J.A., 1936. Improving the technique of the Feulgen stain. Stain Tech. 11, 137–144.

Dionisi, O., Galeotti, T., Terranova, T., Azzi, A., 1975. Superoxide radicals and hydrogen peroxide formation in mitochondria from normal and neoplastic tissues. Biochem. Biophys. Acta 403, 292–300.

Duijndam, W.A.L., Van Duijn, P., 1975. The influence of chromatin compactness on the stoichiometry of the Feulgen-Schiff procedure studied in model films containing condensed or swollen chicken erythrocyte nuclei. J. Histochem. Cytochem. 23, 891–900.

Ervin, E., Jamison, J.M., Gilloteaux, J., Docherty, J.J., Summers, J.L 1998. Characterization of the early events in Vitamin C and K_3-induce death of human bladder tumor cells. Scanning 20, 210–211.

Farber, J.L., Kyle, M.E., Coleman, J.B., 1990. The mechanisms of ce injury by activated oxygen species. Lab. Invest. 62, 670–679.

Freedman, R.S., Pihl, E., Kusyk, C., Gallagher, H.S., Rutledge, F., 197 Characterization of an ovarian carcinoma cell line. Cancer 42, 2352 2359.

Gilloteaux, J., Jamison, J.M., Vijayalaksmi, M., Giammar, D., Summers J.L., 1995. SEM and TEM aspects of synergistic antitumor activit of Vitamin C–Vitamin K_3 combinations against human prostatic ca cinoma cells. Scanning Microsc. Int. 9, 159–173.

Gilloteaux, J., Jamison, J.M., Arnold, D., Ervin, E., Eckroat, L., Docherty J.J., Neal, D., Summers, J.L., 1998a. Cancer cell necrosis by au toschizis: synergism of antitumor activity of Vitamin C:Vitamin K_3 o human bladder carcinoma T24 cells. Scanning 20, 564–575.

Gilloteaux, J., Jamison, J.M., Ervin, E., Taper, H.S., Summers, J.L., 1998b SEM and TEM aspects of the synergistic antitumor activity of Vitami C/Vitamin K_3 combinations against human T24 bladder carcinoma another kind of cell death? Scanning 20, 208–210.

Gilloteaux, J., Jamison, J.M., Venugopal, M., Giammar, D., Summers J.L., 1998c. Synergistic antitumor activity of Vitamin C:Vitamin K combinations against human bladder carcinoma T24 cells: a new cel death by autoschizis. ISPO '98. Cancer Detect. Prevent. 22 (Suppl. 1) S-73.

Gilloteaux, J., Jamison, J.M., von Greunigen, V.E., Arnold, D., Summers J.L., 1999. Autoschizis in ovarian carcinoma cells MDAH as a resul of treatment by combined Vitamin C and K_3 treatment. Scanning 22 119–120.

Gilloteaux, J., Jamison, J.M., Arnold, D., Summers, J.L., 2001a. Au toschizis: another cell death for cancer cells induced by oxidativ stress. In: Motta, P.M., Machiarelli, G., Nottola, S.A. (Eds.), Advance in Microanatomy of Cells and Tissues, Roma. Ital. J. Anat. Embryol 106 (Suppl. 1), 79–91.

Gilloteaux, J., Jamison, J.M., Arnold, D., Taper, H.S., Summers, J.L. 2001b. Ultrastructural aspects of autoschizis: a new cancer cell death induced by the synergistic action of ascorbate/menadione on humar bladder carcinoma cells. Ultrastruct. Pathol. 25, 183–192.

Gilloteaux, J., Jamison, J.M., Arnold, D., von Greunigen, V.E., Summers J.L., 2001c. Autoschizic death of human ovarian carcinoma (MDAH 2774) cells: LM and SEM aspects. Microsc. Microanal. 7 (Suppl. 2: Proc.), 586–587.

Gilloteaux, J., Jamison, J.M., Summers, J.L., 2001d. Cell death by autoschizis in human carcinoma cell lines: nucleus, DNA detection and degradation. Mol. Cell. Biol. 12, 497a.

Gilloteaux, J., Jamison, J.M., Arnold, D., Taper, H.S., von Greunigen. V.E., Summers, J.L., 2003a. Microscopic aspects of autoschizic cell death in human ovarian carcinoma (2774) cells following Vitamin C. Vitamin K_3 or VitaminC:K_3 treatment. Microsc. Microanal. 9, 311–329.

Gilloteaux, J., Jamison, J.M., Arnold, D., Von Greuningen, V., Summers. J.L., 2003b. Autoschizis of human ovarian carcinoma cells: SEM and LM of a new cell death induced by sodium ascorbate:menadione treatment. Scanning 25, 137–149.

Hinshaw, D.B., Skalar, L.A., Bohl, B., Schraufstatter, I.U., Hyslop, P.A., Rossi, M.W., Spragg, R.G., Cochrane, C.G., 1986. Cytoskeletal and morphological impact of cellular oxidant injury. Am. J. Pathol. 123, 454–464.

Ishida, R., Takahashi, T., 1975. Increased DNA chain breakage by combined action of bleomycin and superoxide radical. Biochem. Biophys. Res. Commun. 66, 1432–1438.

Jamison, J.M., Gilloteaux, J., Venugopal, M., Koch, J.A., Shah, R., Summers, J.L., 1996. Flow cytometric and ultrastructural aspects of the synergistic antitumor activity of Vitamin C–Vitamin K_3 combinations against human prostate carcinoma cells. Tissue Cell 28, 687–701.

Jamison, J.M., Gilloteaux, J., Venugopal, M., Koch, J.A., Nicastro, E., Docherty, J.J., Jasso, J., Summers, J.L., 1997. Vitamin C and K3-induced oxidative stress in human prostate tumor cells: mitochondrial ultrastructural alterations. Microsc. Microanal. 3 (Suppl. 2), 23–24.

Jamison, J.M., Gilloteaux, J., Taper, H.S., Summers, J.L., 2001. Evaluation of the in vitro and in vivo antitumor activities of Vitamin C and Vitamin K3 combinations against human prostate cancer. J. Nutr. 131, 158S–160S.

Jamison, J.M., Gilloteaux, J., Taper, H.S., Calderon, P.B., Summers, J.L., 2002. Autoschizis: a novel cell death. Biochem. Pharmacol. 63, 1773–1783.

Jamison, J.M., Gilloteaux, J., Nassiri, M.R., Venugopal, M., Neal, D.R., Summers, J.L., 2004. Cell cycle arrest and autoschizis in a human bladder carcinoma cell line following Vitamin C and Vitamin K_e treatment. Biochem. Pharmacol. 67, 337–351.

Jarabak, R., Jarabak, J., 1995. Effect of ascorbate on the DT-diaphorase-mediated redox cycling of 2-methyl-1,4-naphthoquinone. Arch. Biochem. Biophys. 318, 418–423.

Jemal, A., Murray, T., Samuels, A., Ghafoor, A., Ward, E., Thun, M., 2003. Cancer statistics. CA Cancer J. Clin. 53, 5–26.

Karnovsky, M.J., 1967. The ultrastructural basis of capillary permeability studied with peroxidase as a tracer. J. Cell Biol. 35, 213–236.

Keller, J.M., Cable, S., el Bouhtoury, F., Heusser, S., Scotto, C., Armbruster-Ciolek, E., Colin, S., Schilt, J., Dauca, M., 1993. Peroxisome through cell differentiation and neoplasia. Biol. Cell 77, 77–88.

Koch, C.J., Biaglow, J.E., 1978. Toxicity, radiation sensitivity modification, and metabolic effects of dehydroascorbate and ascorbate in mammalian cells. J. Cell Physiol. 94, 299–306.

Lesko, S.A., Lorentzen, R.J., Ts'o, P.O., 1980. Role of superoxide in deoxyribonucleic acid strand scission. Biochemistry 24, 3023–3028.

Leung, P.Y., Miyashita, K., Young, M., Tsao, C.S., 1993. Cytologic effect of ascorbate and its derivatives on cultured malignant and nonmalignant cell lines. Anticancer Res. 13, 475–480.

Lupulescu, A., 1991. Vitamin C inhibits DNA, RNA and protein synthesis in epithelial neoplastic cells. Int. J. Vitam. Nutr. Res. 61, 125–129.

Lupulescu, A., 1992. Ultrastructure and cell surface studies of cancer cells following Vitamin C administration. Exp. Toxicol. Pathol. 44, 3–9.

Malorni, W., Iosi, F., Mirabelli, F., Belomo, G., 1991. Cytoskeleton as a target in menadione-induced oxidative stress in cultured mammalian cells: alterations underlying surface blebs formation. Chem. Biol. Interact. 80, 217–235.

Maraldi, N.M., Zini, N., Santi, S., Ognibene, A., Rizzoli, R., Mazzoti, G., Manzoli, F.A., 1998. Cytochemistry of the functional domains of the nucleus in normal and in pathologic conditions. Eur. J. Histochem. 42, 41–53.

Minamitsuji-Mochizuki, C., Mitaka, T., Kojima, T., Niitsu, Y., Mochizuki, Y., 1999. Spontaneous appearance of circular actin bands in cultured hepatocytes of adult rats. Med. Electron Microsc. 32, 114–121.

Morgan, A.R., Cone, R.L., Elgert, T.M., 1976. The mechanism of DNA strand breakage by Vitamin C and superoxide and the protective roles of catalase and superoxide dismutase. Nucleic Acids Res. 3, 1139–1149.

Ngo, E.O., Sun, T.P., Chang, J.Y., Wang, C.C., Chi, K.H., Cheng, A.L., Nutter, L.M., 1991. Menadione-induced DNA damage in a human tumor cell line. Biochem. Pharmacol. 42, 1961–1968.

Noto, V., Taper, H.S., Yi-Hua, J., Janssens, J., Bonte, J., De Loecker, W., 1989. Effects of sodium ascorbate (Vitamin C) and 2-methyl-1,4-naphtoquinone (Vitamin K_3) treatment on human tumor cell growth in vitro. Cancer 63, 901–906.

Nutter, L.M., Cheng, A.L., Hung, H.I., Hsieh, R.K., Ngo, E.O., Liu, T.W., 1991. Menadione: spectrum of anticancer therapy and effects on nucleoside metabolism in human neoplastic cell lines. Biochem. Pharmacol. 41, 1283–1292.

Pearse, A.G.E., 1985. Histochemistry, Theoretical and Applied, 4th ed. Churchill Livingstone, Edinburgh, pp. 620–656.

Pething, R., Gascoyne, P.R.C., McLaughlin, J.A., Szent-Györgyi, A., 1983. Ascorbate–quinone interactions: electrochemical, free radical and cytotoxic properties. Proc. Natl. Acad. Sci. U.S.A. 80, 129–132.

Prasad, K.N., Edwards-Prasad, J., Sakamoto, A., 1979. Vitamin K_3 (Menadione) inhibits the growth of mammalian tumor cells in culture. Life Sci. 29, 1387–1392.

Ricchiuti, D.J., Iturregui, J., Neal, D.R., Jamison, J.M., Gilloteaux, J., Summers, J.L., 2003. Toxic Effects of Vitamin C and Synthetic Vitamin K_3 (Menadione) Combinations over the Life Spans of C3H Inbred Mice, North Central Section American Urology Association Meeting, Vancouver, BC, 20 September 2003.

Ries, L.A., 1993. Ovarian cancer—survival and treatment differences by age. Cancer 71, 524–529.

Riordan, N.H., Riordan, H.D., Meng, X., Li, Y., Jackson, J.A., 1995. Intravenous ascorbate as a tumor cytotoxic chemotherapeutic agent. Med. Hypothesis 44, 207–213.

Sakagami, H., Satoh, K., 1997. Modulating factors of radical intensity and cytotoxic activity of ascorbate (review). Anticancer Res. 17, 3513–3520.

Sambrook, R.J., Fritsch, E.F., Maniatis, T., 1989. Molecular Cloning, 2nd ed. Cold Spring Harbor Laboratory, Cold Spring Harbor, NY.

Sanger, J.W., Sanger, J.M., 1983. Differential response of three types of actin filament bundles to depletion of cellular ATP levels. Eur. J. Cell Biol. 31, 197–204.

Taper, H.S., 1967. L'activité des nucléases et phosphatases acides et alcalines dans les tumeurs rénales induites chez le rat par la diméthylnitrosamine (Etude histochimique). Path. Eur. 2, 406–420.

Taper, H.S., 1980. Reversibility of acid and alkaline deoxyribonuclease deficiency in malignant tumor cells. J. Histochem. Cytochem. 29, 1053–1060.

Taper, H.S., Fort, L., Brucher, J.M., 1971. Histochemical activity of alkaline and acid nucleases in rat liver parenchyma during *N*-nitrosomorpholine carcinogenesis. Cancer Res. 31, 913–916.

Taper, H.S., de Gerlache, J., Lans, M., Roberfroid, M., 1987. Non-toxic potentiation of cancer chemotherapy by combined C and K_3 vitamin pretreatment. Int. J. Cancer 40, 575–579.

Tsao, C.S., Dunham, W.B., Leung, P.Y., 1988. In vivo antineoplastic activity of ascorbic acid for human mammary tumor. In Vivo 2, 147–150.

Taper, H.S., Keyeux, A., Roberfroid, M., 1996. Potentiation of radiotherapy by nontoxic pretreatment with combined Vitamin C and K_3 in mice bearing solid, transplantable tumor. Anticancer Res. 16, 499–504.

Taper, H.S., Jamison, J.M., Gilloteaux, J., Gwin, C.A., Gordon, T., Summers, J.L., 2001. In vivo reactivation of DNases in implanted human prostate tumors after administration of a Vitamin C/K_3 combination. J. Histochem. Cytochem. 49, 109–119.

Varga, J.M., Airoldi, L., 1983. Inhibition of transplantable melanoma tumor development in mice by prophylactic administration of Ca-ascorbate. Life Sci. 32, 1559–1964.

Venugopal, M., Jamison, J.M., Gilloteaux, J., Koch, J.A., Summers, M., Hoke, J., Sowick, C., Summers, J.L., 1996a. Synergistic antitumor reactivity of Vitamins C and K_3 against human prostate carcinoma cell lines. Cell Biol. Int. 20, 787–797.

Venugopal, M., Jamison, J.M., Gilloteaux, J., Koch, J.A., Summers, M., Giammar, D.M., Sowick, C., Summers, J.L., 1996b. Synergistic antitumor activity of Vitamin C and K_3 on human urologic tumor cell lines. Life Sci. 59, 1389–1400.

Von Gruenigen, V.E., Jamison, J.M., Gilloteaux, J., Lorimer, H.E., Summers, M., Pollard, R.R., Gwin, C.A., Summers, J.L., 2003. The in vitro antitumor activity of Vitamins C and K-3 against ovarian carcinoma. Anticancer Res. 23, 3279–3287.

Wu, F.Y., Chang, N.T., Chen, W.J., Juan, C.C., 1993a. Vitamin K3-induced cell cycle arrest and apoptotic cell death are accompanied by

altered expression of *c-fos* and *c-myc* in nasopharyngeal carcinoma cells. Oncogene 8, 2237–2244.

Wu, F.Y., Liao, W.C., Chang, H.M., 1993b. Comparison of antitumor activity of Vitamins K1, K2 and K3 on human tumor cells by two (MTT and SRB) cell viability assays. Life Sci. 52, 1797–1804.

Yamafuji, K., Nakamura, Y., Omura, H., Soeda, T., Gyotoku, K., 1971. Antitumor potency of ascorbic acid, dehydroascorbic or 2,3-diketogulonic acid and their action on deoxyribonucleic acid. Z. Krebsforsch. Onkol. Cancer Res. Clin. Oncol. 76, 1–7.

Yang, I., Chew, E.C., Chew-Cheng, S.B., Jiao, R.J., Yam, H.F., Zhai, Z.H., 1994. Fine structural observation of a nucleolar-nuclear matrix-lamina-intermediate filament system in transformed cells. Anticancer Res. 14, 1829–1832.

Zhang, W., Negoro, T., Satoh, K., Jiang, Y., Hashimoto, K., Kikuchi, H., Nishikawa, H., Miyata, T., Yamamoto, Y., Nakano, K., Yasumoto, E., Nakayachi, T., Mineno, K., Satoh, T., Sakagami, H., 2001. Synergistic cytotoxic action of Vitamin C and Vitamin K3. Anticancer Res. 21, 3439–3444.